Rapidity dependence of the proton-to-pion ratio in Au+Au and p+p collisions at $\sqrt{s_{NN}} = 62.4$ and 200 GeV[☆]

I. G. Arsene[j,3], I. G. Bearden[d], D. Beavis[a], S. Bekele[i,4], C. Besliu[h], B. Budick[c], H. Bøggild[d], C. Chasman[a], C. H. Christensen[d], P. Christiansen[d,5], H. H. Dalsgaard[d], R. Debbe[a], J. J. Gaardhøje[d], K. Hagel[f], H. Ito[a], A. Jipa[h], E. B. Johnson[i,8], C. E. Jørgensen[d,6], R. Karabowicz[e], N. Katryńska[e], E. J. Kim[a,i,7], T. M. Larsen[j], J. H. Lee[a], G. Løvhøiden[j], Z. Majka[e], A. Marcinek[e], M. J. Murray[f,i], J. Natowitz[f], B. S. Nielsen[d], C. Nygaard[d], D. Pal[i], A. Oviller[j], R. Płaneta[e], F. Rami[b], C. Ristea[d], O. Ristea[h], D. Röhrich[g], S. J. Sanders[i], P. Staszel[e,1], T. S. Tveter[j], F. Videbæk[a,2], R. Wada[f], H. Yang[g,9], Z. Yin[g,10], and I. S. Zgura[h]

[a]Brookhaven National Laboratory, Upton, New York 11973
[b]Institut Pluridisciplinaire Hubert Curien CRNS-IN2P3 et Université Louis Pasteur, Strasbourg, France
[c]New York University, New York 10003
[d]Niels Bohr Institute, Blegdamsvej 17, University of Copenhagen, Copenhagen 2100, Denmark
[e]Smoluchowski Inst. of Physics, Jagiellonian University, Kraków, Poland
[f]Texas A&M University, College Station, Texas, 77843
[g]University of Bergen, Department of Physics and Technology, Bergen, Norway
[h]University of Bucharest, Romania
[i]University of Kansas, Lawrence, Kansas 66045
[j]University of Oslo, Dep. of Physics, Blindern, 0316 Oslo, Norway

Abstract

The proton-to-pion ratios measured in the BRAHMS experiment for Au+Au and p+p collisions at $\sqrt{s_{NN}} = 62.4$ and 200 GeV are presented as a function of transverse momentum and collision centrality at selected pseudorapidities in the range of 0 to 3.8. A strong pseudorapidity dependence of these ratios is observed. We also compare the magnitude and p_T-dependence of the p/π^+ ratios measured in Au+Au collisions at $\sqrt{s_{NN}} = 200$ GeV and $\eta \approx 2.2$ with the same ratio measured at $\sqrt{s_{NN}} = 62.4$ GeV and $\eta = 0$. The great similarity found between these ratios throughout the whole p_T range (up to 2.2 GeV/c) is consistent with particle ratios in A+A collisions being described with grand-canonical distributions characterized by the baryo-chemical potential μ_B. At the collision energy of 62.4 GeV, we have observed a unique point in pseudorapidity, $\eta = 3.2$, where the p/π^+ ratio is independent of the collision system size in a wide p_T-range of $0.3 \leq p_T \leq 1.8$ GeV/c.

Key words: heavy ion collision, particle ratios, forward rapidity, hadronization
PACS: 25.75.q, 25.75.Dw, 25.40.-h, 13.75.-n

1. Introduction

The ongoing dialogue between theory and experiment is delivering an increasingly clear picture of the QCD phase diagram in its partonic and hadronic phases. In particular, recent mid-rapidity RHIC results are considered as evidence for a smooth cross over from a dense

[☆]The BRAHMS Collaboration
[1]Corresponding author. Email: ufstasze@if.uj.edu.pl
[2]Spokesperson. Email: videbaek@bnl.gov
[3]Current Address: ExtreMe Matter Institute EMMI, GSI Helmholtzzentrum für Schwerionenforschung GmbH, Darmstadt, Germany
[4]Current Address: Dept of Physics, Tennessee Tech University,Cookeville, Tennessee 38505
[5]Current Address: Div. of Experimental High-Energy Physics, Lund University, Lund, Sweden
[6]Risø National Laboratory, Denmark
[7]Current Address : Division of Science Education, Chonbuk National University, Jeonju, 561-756, Korea
[8]Current Address: Radiation Monitoring Devices, Cambridge, Massachusetts
[9]Current Address: Physics Institute, University of Heidelberg, Heidelberg, Germany
[10]Current Address: Institute of Particle Physics, Huazhong Normal University, Wuhan, China

and opaque partonic phase into a hadronic gas at temperatures around 170 MeV and small values of baryo-chemical potential μ_B [1]. Measurements of the relative abundances of hadronic species constrain statistical models used to describe the chemical freeze-out in nucleus-nucleus interactions at different energies. Some of these models show a remarkable behavior at low baryo-chemical potential where the curves of temperature vs. baryo-chemical potential representing chemical freeze-out tend to merge with the phase boundary between partonic and hadronic media [2]. In such a picture, hadrons are produced very close to freeze-out, and one could safely state that the features of the partonic medium are transmitted to the final bulk hadrons via hadronization processes. Indeed, such appears to be the case for the constituent quark scaling found in elliptic flow v_2 measurements [3] as well as the enhancement of baryon-to-meson ratios that scale with the collision size around mid-rapidity (low μ_B) [4, 5]. This increase in the baryon-to-meson ratios (≈ 1 for the so-called intermediate p_T values ranging from 2 to 6 GeV/c), first reported by the PHENIX collaboration [6], deviates remarkably from calculations that include parton fragmentation in the vacuum. The p_T-dependence of the baryon-to-meson ratio in the intermediate p_T range appears to be related to a modification of hadronization in the partonic medium created by the collision. This effect could be caused by the different quark content of the baryons and mesons [7] or because of their different masses through the effect of radial flow [8].

Both radial flow and in-medium quark coalescence are expected to enhance protons over pions at intermediate p_T. In particular, the PHENIX $\bar{p}/\pi^-$ data at mid-rapidity is well described by the Greco, Ko, and Levai quark coalescence model [9] where the introduced coalescence involves partons from the medium (thermal) and partons from mini-jets. The Hwa and Yang quark recombination model [10] describes well the BRAHMS and PHENIX p/π^+ ratios around mid-rapidity. These mid-rapidity results are consistent with hadronization in the intermediate p_T range being dominated by parton recombination with negligible final state interactions between the produced hadrons. In contrast, at forward rapidity (large μ_B), a significant gap between the temperature of the transition from the partonic to the hadronic phase, T_c, and the temperature of chemical freeze-out is predicted by QCD lattice calculation [11]. In that environment, hadronic re-scattering may play an important role, making statistical models more suitable to describe particle abundances at high rapidity [12, 13].

We present in this letter the p/π ratios for both charges extracted from Au+Au collisions at different centralities as well as p+p at $\sqrt{s_{NN}} = 62.4$ and 200 GeV. The ratios are presented as function of pseudorapidity and transverse momentum p_T. The system size dependence of the ratios is investigated and compared to the smallest system; p+p collisions. The comparison of the p/π^+ measured at two different energies and pseudorapidities is used to establish a connection between particle abundances in these systems and their possible description by a grand-canonical distribution. We also present an interesting feature in the pseudorapidity dependence of the p/π^+ ratio at $\sqrt{s_{NN}} = 62.4$ GeV. There the ratio has the same magnitude and p_T dependence at $\eta = 3.2$ when measured at all Au+Au centralities as well as p+p collisions. We compare the ratios extracted from the most central Au+Au events to a hydrodynamical model and to a partonic cascade model that includes hadronic re-scattering in the final state.

2. Experimental setup

The BRAHMS detector setup [14] consists of two movable, small acceptance spectrometers: the Mid-Rapidity Spectrometer (MRS), which operates in the polar angle interval from $90^\circ \geq \theta \geq 30^\circ$ (corresponding to a pseudorapidity interval of $0 \leq \eta \leq 1.3$) and the Forward Spectrometer (FS), which operates in the range from $15^\circ \geq \theta \geq 2.3^\circ$ ($2 \leq \eta \leq 4$). The BRAHMS setup also includes detectors used to determine global features of the collision such as the overall charged particle multiplicity, the collision vertex and the centrality of the collision. The MRS is composed of a single dipole magnet placed between two Time Projection Chambers (TPC), which provide a momentum measurement. Particle identification (PID) is based on Time-of-Flight (TOF) measurements [14]. The FS has two TPCs, which are capable of track recognition in a high multiplicity environment close to the interaction region, and, at the far end of the spectrometer, three Drift Chambers. In the aggregate, the FS can detect particle track segments with high momentum resolution ($\delta p/p = 0.0008p$ at the highest field setting) using three dipole magnets. Particle identification in the FS is provided by TOF measurements in two separate hodoscopes for low and medium particle momenta, respectively. High momentum particles are identified using a Ring Imaging Cherenkov detector (RICH) [15].

3. The analysis

The analysis reported in this letter consists of the comparison of proton and pion yields as a function of

p_T for several pseudorapidity intervals. The analysis is carried out in η versus p_T space, since for any given angle and field configuration the acceptance is the same for pions and protons. For a given η-p_T bin the p/π ratios are calculated on a setting by setting basis. In order to avoid mixing different PID techniques, which can lead to different systematic uncertainties, the ratios are calculated separately for PID using TOF and the RICH detectors. In this way, all factors such as acceptance corrections, tracking efficiencies, trigger normalization and bias related to the centrality cut cancel out in the ratio. The remaining species dependent corrections are:

(i) decays in flight and interactions with the beam pipe and other material, and
(ii) the PID efficiency correction.

The corrections for (i) are determined from the single particle response of pions and protons with energy in a realistic GEANT [16] model description of the BRAHMS experimental setup. The magnitude of this correction on the particle ratios depends on the particle momenta and the spectrometer positions, but does not exceed 6%. We estimate that the overall systematic uncertainty related to this correction is at the level of 2%.

The TOF PID is done separately for small momentum bins by fitting a multi-Gaussian function to the experimental squared mass m^2 distribution and applying a $\pm 3\sigma$ cut to select a given particle type. For measurements done with the FS spectrometer in the momentum range where pions overlap with kaons (usually above 3.5 GeV/c), the RICH detector can be used in veto mode to select kaons with momentum smaller than the kaon Cherenkov threshold, which is about 9 GeV/c. This procedure leads to a relatively clean sample of pions with some contamination by kaons having spurious rings associated in the RICH counter. Together with the kaon - proton overlap at larger momenta, this contamination effect is a source of systematic errors which have been estimated to be in the order of a few percent for all p_T values, except for low $p_T$in the $\bar{p}/\pi^-$ ratios, where these uncertainties can reach high values ($\approx$ 15%). At mid-rapidity the systematic uncertainty reaches a value of 5% at $p_T > 2.5$ GeV/c due to the limited kaon to pion separation at large momenta.

The RICH PID is also based on the particle separation in the m^2 versus momentum space. The RICH provides direct proton identification above the proton threshold momentum which is about 15 GeV/c. However, an additional proton identification scheme is possible below this value but above the kaon threshold. In this momentum range a proton is associated with tracks having momenta above the kaon threshold, but no RICH signal (veto mode). The veto proton yields are corrected for pion and kaon contamination due to a small RICH inefficiency. The RICH inefficiency was determined by studying yields of tracks identified in the TOF detector as pions but having no ring associated in the RICH. This study was done for a low momentum range with a good kaon/pion separation in TOF. It is found that the pion inefficiency is equal to unity at the pion threshold ($\approx$ 2.3 GeV/c) and rapidly decreases at larger momenta reaching a constant value of about 3% around 4 GeV/c. The RICH inefficiency found for pions is then applied to kaons (and the other species) assuming that Cherenkov radiation depends only on the γ factor of the particle. A more detailed description of the RICH inefficiency analysis is given in [15] and a forthcoming publication. There are two sources of systematic uncertainties associated with the RICH PID, namely, the uncertainty on the RICH inefficiency, estimated to be at the level of 10%, and the overlap in m^2 between pions and kaons having momenta above about 30 GeV/c.

No corrections were applied for weak decays. However we apply cuts on track and event vertex matching to limit the effects of feed down on particle yields. The range of the cut is related to the uncertainty of the particle track projection to the event vertex. Using AMPT [17] model calculations we found that these vertex cuts lead to remnant contamination of proton and pion yields mainly due to Λ hyperons and K_s^0 meson decays. At mid-rapidity we estimated that this contamination leads to a 10%(7%) enhancement of $p/\pi^+(\bar{p}/\pi^-)$ at p_T = 3.0 GeV/c. This enhancement increases toward low transverse momenta and reaches 20%(14%) for $p/\pi^+(\bar{p}/\pi^-)$ at p_T = 1.5 GeV/c. The level of contamination decreases gradually towards forward rapidities and at $\eta \approx 3$ the enhancement reaches values of 6%(5%) for $p/\pi^+(\bar{p}/\pi^-)$ at p_T = 3.0 GeV/c and 10%(7%) for $p/\pi^+(\bar{p}/\pi^-)$ at p_T = 1.5 GeV/c.

4. Results

Figure 1 shows p/π^+ ratios measured in Au+Au collisions at $\sqrt{s_{NN}}$ = 200 GeV in two centrality classes of events, namely, (0 − 10% (solid dots) and 40 − 80% (open squares)). The centrality selection is based on the charged-particle multiplicity measured in the range $-2.2 < \eta < 2.2$ as described in [18]. The shaded boxes, plotted for the most central events, represent the systematic uncertainties discussed in the previous section. The ratios extracted from p+p data at the same energy are plotted for comparison (solid triangles). The p_T coverage depends on the pseudorapidity bins and for central Au+Au collisions extends up to p_T = 4 GeV/c for

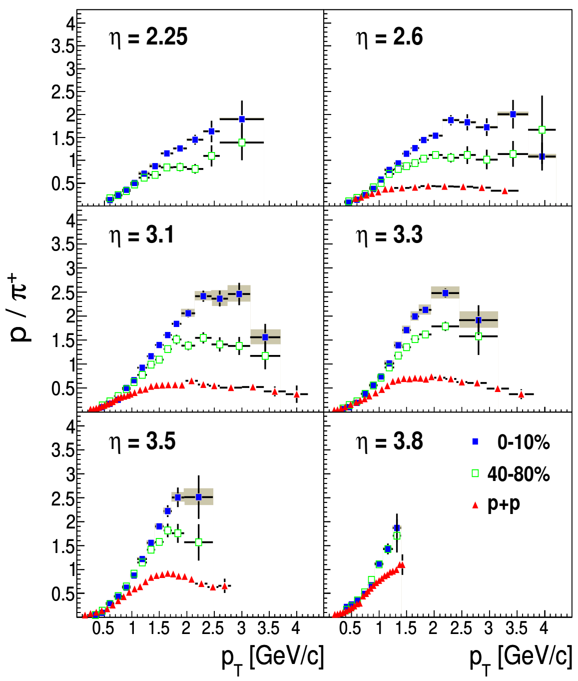

Figure 1: Centrality dependent p/π^{+} ratios for Au+Au system colliding at $\sqrt{s_{NN}}$ = 200 GeV for central (0 – 10%) and semi-peripheral (40 – 80%) reactions in comparison with p+p collision data at the same energy. The vertical bars represent the statistical errors and the shaded boxes (plotted only for central Au+Au) show the systematic uncertainties.

η = 2.6. At low p_T (< 1.5 GeV/c) the p/π^{+} ratios exhibit a rising trend with a weak dependence on centrality. A significant dependence on centrality begins above 1.5 GeV/c. The ratios appear to reach a maximum value at p_T around 2.5 GeV/c wherever the p_T coverage is sufficient to determine this limit. The maxima of the ratios are greater for more central events and, at η = 3.1, are equal to about 2.5 and 1.5 for the 0 – 10% and 40 – 80% centrality bins, respectively. The p+p ratios are consistent with Au+Au data at low p_T and begin to deviate significantly above p_T = 1 GeV/c. At η = 3.1 a maximum value of the ratio of 0.55 is reached in p+p collisions which is a factor of 4.5 smaller than that observed for central Au+Au reactions. We have performed PYTHIA [19] calculations for nucleon-nucleon interactions in each possible isospin state. The calculations of the p/π ratio vs. p_T show no significant dependence on the isospin of the initial NN system. Thus the difference between p+p and Au+Au is not an isospin effect.

The values of the $\bar{p}/\pi^{-}$ ratios plotted in Fig. 2 are significantly lower than the p/π^{+} ratios (note the difference in the vertical scale), however, the centrality dependence shows the same features as those observed in the p/π^{+} ratios, namely, that the ratios for different centrality classes are consistent with each other up to $p_T \approx$ 1.2 GeV/c and a strong dependence on centrality appears at larger transverse momenta reaching a maximum at similar p_T as the positive particles. Looking at the p+p data alone, one notes the difference in shape between the p/π^{+} and $\bar{p}/\pi^{-}$ ratios: a clear shift of the $\bar{p}/\pi^{-}$ peaks towards lower p_T, as well as a much broader p/π^{+} peaks. The large difference between the Au+Au and p+p both in shape and overall magnitude may reflect significant medium effects in Au+Au collisions at $\sqrt{s_{NN}}$ = 200 GeV in the pseudorapidity intervals covered.

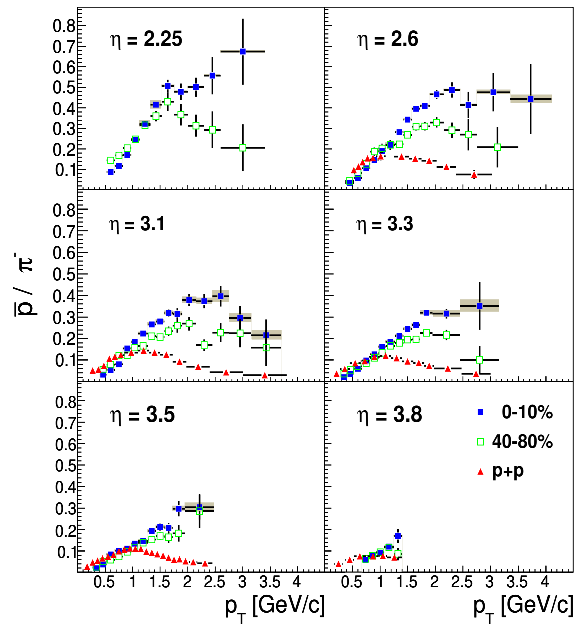

Figure 2: The ratios of $\bar{p}/\pi^{-}$measured in Au+Au and p+p collisions at $\sqrt{s_{NN}}$ = 200 GeV, are plotted for the same centrality samples used in Fig. 1.

In Fig. 3 we explore the possible connection between the measured p/π ratios in extended systems and the baryo-chemical μ_B used to characterize them as statistical systems. Such a connection is done by comparing two rapidity ranges that have the same $\bar{p}/p$ ratio but different $\sqrt{s_{NN}}$. These are η = 0 at 62 GeV and η = 2.2 at 200 GeV.

The pseudorapidity intervals selected for this comparison correspond to similar observed $\bar{p}/p$ ratios of approximately 0.45. The very similar $\bar{p}/p$ ratios in these two systems has been attributed to their having a common value of the baryo-chemical potential μ_B of

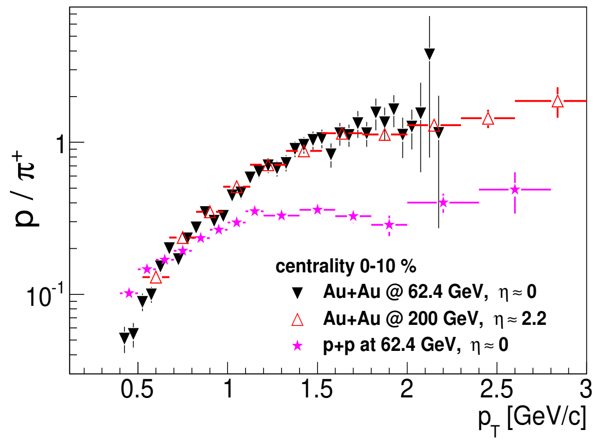

Figure 3: p/π^+ ratio in Au+Au collisions for η = 0.0 at $\sqrt{s_{NN}}$ = 62.4 GeV marked with open triangles and the Au+Au reactions for η = 2.2 at $\sqrt{s_{NN}}$ = 200 GeV marked with the black triangles. Stars shown reference mid-rapidity data for p+p at $\sqrt{s_{NN}}$ = 62.4 GeV.

$\sim$ 62 MeV [20, 21]. The similarity of proton-to-pion ratios for these selected heavy ion collisions suggests that the baryon and meson production at the p_T interval studied (up to 2 GeV/c) is dominated by medium effects and is determined by the bulk medium properties. The considerably lower values of the p/π^+ ratio measured in the p+p system at $\sqrt{s}$ = 200 GeV, shown with stars in Fig. 3, can also be construed as strong indication that medium effects are the source of the observed enhancement of the p/π as function of p_T in the nucleus-nucleus collisions.

The three panels of Fig. 4 display the p/π^+ ratio extracted from p+p and Au+Au collisions at $\sqrt{s_{NN}}$ = 62.4 GeV measured at 3 different pseudorapidity bins; η = 2.67 (top panel), η = 3.2 (middle panel) and η = 3.5 (bottom panel). At η = 2.67, p/π^+ is greater in Au+Au than in p+p collisions while at η = 3.5 the situation is reversed. The middle panel of Fig. 4 shows the p/π^+ ratios from Au+Au and p+p collisions at $\sqrt{s_{NN}}$ = 62.4 GeV at η = 3.2. This "crossing point" in pseudorapidity shows a remarkably complete overlap of the ratios as function of p_T not only for p+p and 0 − 10% central Au+Au reactions, but also for other Au+Au centralities, namely 10 − 20%, 20 − 40% and 40−80%. Such a universal shape for the p/π^+ ratios implies that the nuclear modification factor for protons and pions are consistent with each other at all measured p_T and all centrality at this pseudorapidity. The observed crossing of p/π^+ ratios for different sizes of the colliding systems is consistent with recent BRAHMS results on the centrality dependence of net-proton rapidity dis-

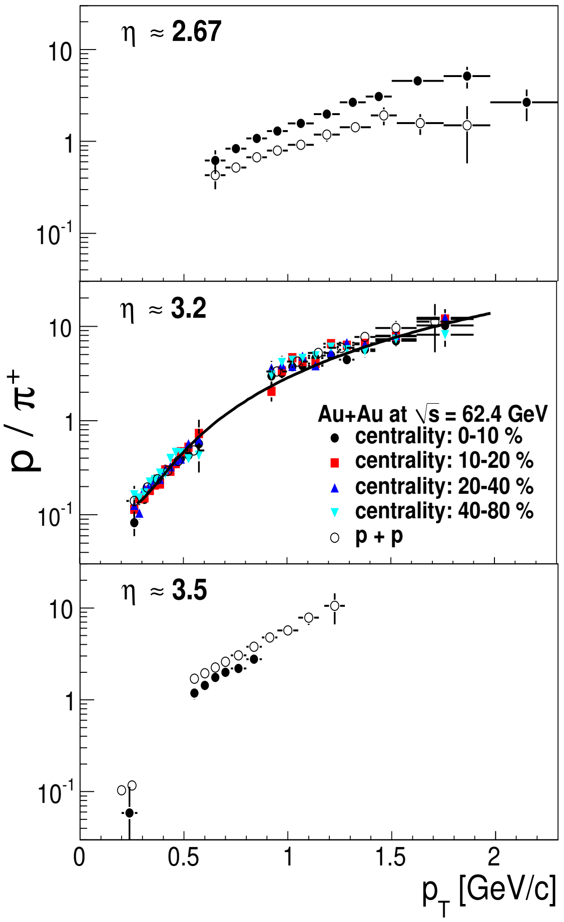

Figure 4: p/π^+ ratio from p+p and Au+Au collisions at $\sqrt{s_{NN}}$ = 62.4 GeV for η = 2.67 (top panel), η = 3.2 (middle panel) and η = 3.5 (bottom panel). The curve drawn in the middle panel is a polynomial fit to the most central events, its purpose is to guide the eye and bridge the gap in p_T .

tribution in Au+Au reactions at $\sqrt{s_{NN}}$ = 200 GeV [22]. The data show an increased baryon transport towards mid-rapidity in central collisions. Such increased stopping power dissipates the beam energy to form a denser system where recombination mechanisms favor proton production at intermediate values of p_T. Both effects will produce higher values of the p/π^+ ratio in larger systems. On the other hand, at very forward rapidities (around one unit below the beam rapidity) a bigger fraction of the measured particles are protons and their numbers are even higher for lighter systems due to reduced stopping power. This observation is consistent with the reversed p/π^+ dependence on the system size seen in the bottom panel. A crossing of p/π^+ yields ratio at the energy of 62.4 GeV is predicted by UrQMD [23], HIJING [24] and AMPT model calculations. However, these models predict the location of the crossing point in the interval $2 < y < 2.5$, which is almost one unit of rapidity lower than the observed value. These experimental results then provide a strong constraint on the theoretical description of baryon number transport and associated energy dissipation in relativistic nuclear reactions. It is worth noting that at 200 GeV (see Fig. 1), even for $\eta = 3.8$, the p/π^+ ratios measured in Au+Au reactions are larger than those observed in p+p collisions, so the possible crossing point at high energy is located at larger rapidity, beyond the experimental acceptance.

5. Model comparisons

To interpret these results, theoretical models of nucleus-nucleus collisions are confronted with the data. The p/π^+ ratio measured in central Au+Au collisions at $\sqrt{s_{NN}} = 200$ GeV, shown on the top row of Fig. 5, has a strong growth with rapidity; starting from a value of about 1.0 at $\eta \approx 0$ and $p_T \approx 3$ GeV/c and reaching a value of 2.5 at $\eta \approx 3.5$ and $p_T \approx 3$ GeV/c. In contrast, the $\bar{p}/\pi^-$ ratio (bottom row) decreases with increasing rapidity (from ≈ 1 at $\eta \approx 0$ to 0.4 at $\eta \approx 3.5$). Note the different vertical scales for positive and negative charged particles. Figure 5 compares our results for $0-10\%$ central Au+Au reactions at $\sqrt{s_{NN}} = 200$ GeV to two model calculations based on: the THERMINATOR model [25] (black dashed lines) and the AMPT model (solid lines). THERMINATOR is a 1+1-D hydrodynamic model that incorporates statistical particle production (including excited states), which in turn, has chemical potentials with parameterized rapidity dependence. Alternatively, the AMPT (A Multi-Phase Parton Transport) model includes mini-jet parton production, parton dynamics, hadronization according to the LUND string fragmentation model, and final state hadronic interactions in determining the final particle production. In these simulations we duplicate experimental conditions regarding the particle contamination due to weak decays, the tracks were required to point to the event vertex under the same conditions as those applied to the experimental data.

At forward rapidities the THERMINATOR model tracks well the trends of the data up to $p_T \approx 2.5$ GeV/c for both positive and negative particles. At $\eta = 0$ this model under predicts the experimental p/π^+ and $\bar{p}/\pi^-$ ratios in the intermediate p_T range covered by the data ($1 < p_T < 3$ GeV/c). At large p_T (> 3 GeV/c) THERMINATOR fails to describe the data. The mismatch is clearly seen in the $\eta = 3.05$ plot of Fig. 5, where the data have the best p_T coverage. This mismatch is attributed to the fact that the model does not include the production of jets. The AMPT model can qualitatively describe the pseudorapidity trends, but fails to quantitatively describe the data, namely, the model under predicts p/π^+ and over predicts $\bar{p}/\pi^-$ ratios. We note that the AMPT describes the p/π^+ ratios reasonably well for semi-peripheral reactions (not shown).

6. Summary

We present the p_T-dependence of the p/π ratios measured in Au+Au and p+p collisions at energies of 62.4 and 200 GeV as a function of pseudorapidity and collision centrality. The data provide the opportunity to study baryon-to-meson production over a wide range of the baryo-chemical potential μ_B. For Au+Au collisions at $\sqrt{s_{NN}} = 200$ GeV the p/π^+ and $\bar{p}/\pi^-$ ratios show a noticeable dependence on centrality at intermediate p_T with a rising trend from p+p to central Au+Au collisions. We find that p/π^+ ratios are remarkably similar for central Au+Au at $\eta \approx 2.2$ at $\sqrt{s_{NN}} = 200$ GeV, and central Au+Au at $\eta \approx 0$ at $\sqrt{s_{NN}} = 62.4$ GeV, where the bulk medium is characterized by the same value of $\bar{p}/p$. This observation, together with the observed centrality dependence suggests that particle production for intermediate p_T values is governed by the size and the chemical properties of the created medium for the systems and pseudorapidity range studied. It is also shown that the statistical model confronted with the data, under predicts the mid-rapidity p/π^+ and $\bar{p}/\pi^-$ ratios for central Au+Au at $\sqrt{s_{NN}} = 200$ GeV, but describes well the data trends at high rapidity. Finally, the Au+Au and p+p measurements at $\sqrt{s_{NN}} = 62.4$ GeV show that the p/π^+ ratios for p+p and for all analyzed Au+Au centralities cross simultaneously at the same η value (≈ 3.2) and are consistent with each other in the covered p_T range, e.g., from 0.3 GeV/c up to 1.8 GeV/c.

Acknowledgments

This work was supported by the Division of Nuclear Physics of the Office of Science of the U.S. Department of Energy under contracts DE-AC02-98-CH10886, DE-FG03-93-ER40773, DE-FG03-96-ER40981, and DE-FG02-99-ER41121, the Danish Natural Science Research Council, the Research Council of Norway, the Polish Ministry of Science and Higher Education (Contract no 1248/B/H03/2009/36), and the Romanian Ministry of Education and Research (5003/1999, 6077/2000), and a sponsored research grant from Renaissance Technologies Corp. We thank the staff of the

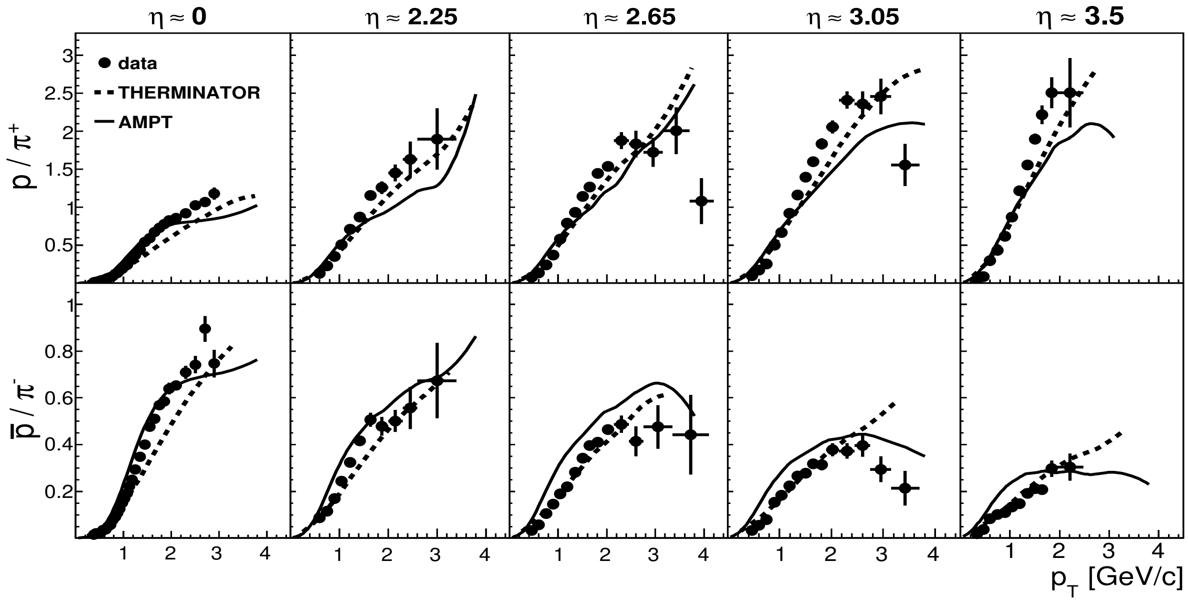

Figure 5: Rapidity evolution of p/π^+ and $\bar{p}/\pi^-$ for 0 − 10% central Au+Au reaction at $\sqrt{s_{NN}}$ = 200 GeV (solid points), and calculations from the THERMINATOR (dashed line) and the AMPT models (solid line).

Collider-Accelerator Division and the RHIC computing facility at BNL for their support to the experiment.

References

[1] M. Stephanov, XXIV International Symposium on Lattice Field Theory, Tucson, Arizona, USA, July 23-28, 2006, Z. Fodor, arXiv:0712.2930v1 [hep-lat].

[2] P. Braun-Munzinger, Nucl. Phys. **A 681**, 119c-123c (2001).

[3] R. A. Lacey, and A. Taranenko, The 2nd Edition of International Workshop - Correlations and Fluctuations in Relativistic Nuclear Collisions, Galileo Galilei Institute, Florence, Italy, July 7-9, 2006; R. A. Lacey *et al.*, Phys. Rev. Lett. **98**, 092301 (2007) [arXiv:nucl-ex/0609025].

[4] E. J. Kim (BRAHMS Collaboration), Nucl. Phys. **A 774**, 493 (2006).

[5] R. Debbe (BRAHMS Collaboration) J.Phys. G: Nucl. Part. Phys. **35**, 104004 (2008).

[6] K. Adcox et al., [PHENIX Collaboration], Phys. Rev. Lett. **88**, 242301 (2002).

[7] R. J. Fries et al., Phys. Rev. Lett. **90**, 202303 (2003); S. A. Bass, J. Phys. Conf. Ser. **50**, 279 (2006).

[8] T. Peitzmann, Nucl. Phys. **A 727**, 179 (2003).

[9] V. Greco, C.M. Ko, and P. Levai, Phys. Rev. Lett. **90**, 022302 (2003).

[10] R. C. Hwa, and C. B. Yang, Phys. Rev. **C 67**, 034902 (2003).

[11] P. Braun-Munzinger, J. Stachel, Jour. of Phys. **G 28**, 1971 (2002).

[12] T. Hirano, and Y. Nara, Nucl. Phys. **A 743**, 305 (2004); T. Hirano, and Y. Nara, Phys. Rev. **C 69**, 034908 (2004).

[13] W. Broniowski, and W. Florkowski, Phys. Rev. Lett. **87**, 272302 (2001).

[14] M. Adamczyk et al., [BRAHMS Collaboration], Nucl. Instr. Meth. **A 499**, 437 (2003).

[15] R. Debbe et al., Nucl. Instr. Meth. **A 570**, 216 (2007).

[16] GEANT3, CERN program library.

[17] Z. W. Lin et al., Phys. Rev. **C 72**, 064901 (2005).

[18] I.G. Bearden et al. [BRAHMS Collaboration], Phys. Rev. Lett. **88**, 202301 (2002).

[19] T. Sjostrand, Comp. Phys. Commun. **82**, 74 (1994); Version 6.4. T. Sjostrand, S. Mrenna, and P. Skands, JHEP **05**, 026 (2006); http://www.thep.lu.se/tf2/staff/torbjorn/Pythia.thml.

[20] I.G. Bearden et al. [BRAHMS Collaboration], Phys. Rev. Lett. **90**, 102301 (2003).

[21] I.C. Arsene et al., for BRAHMS Collaboration, Int. Jour. of Mod. Phys.**E 16**, 2035 (2007), I.C. Arsene [for the BRAHMS Collaboration], IJMPE **16**, (2007) 2035.

[22] F Videbæk, Quark Matter 2009, Knoxville, USA, April 2009, BRAHMS plenary talk arXiv:0907.4742 [nucl-ex].

[23] M. Bleicher et al., J. Phys. G: Part. Phys. **25**, 1859 (1999).

[24] M. Gyulassy and X.N. Wang Comput. Phys. Commun. **83**, 307 (1994).

[25] W. Broniowski, and B. Biedroń, Phys. Rev. **C 75**, 054905 (2007).